Proceedings Paper:

Gu, X and Zhang, LX (2014) Symbol Synchronization for OFDM based Heterogeneous Network in the Presence of Co-channel Interference. In: Communications and Networking in China (CHINACOM), 2014 9th International Conference on. 9th International Conference on Communications and Networking in China (CHINACOM), 14-16 Aug 2014, Maoming, China. Institute of Electrical and Electronics Engineers , 220 - 225. ISBN 978-1-4799-5970-9

https://doi.org/10.1109/CHINACOM.2014.7054289

Symbol Synchronization for OFDM based Heterogeneous Network in the Presence of Co-channel Interference

Xuan Gu
School of Electronic and Electrical Engineering
University of Leeds
Leeds, UK
Email: elxg@leeds.ac.uk

Li Zhang
School of Electronic and Electrical Engineering
University of Leeds
Leeds, UK
Email: l.x.zhang@leeds.ac.uk

***Abstract*—This paper explores the symbol synchronization in the presence of co-channel interference (CCI) of Orthogonal Frequency Division Multiplexing (OFDM) based heterogeneous network (HetNet). The CCI is generated by a HetNet model with macrocell and small cells. Schmidl and Cox (S&C) Algorithm is applied for symbol synchronization. We find that the presence of CCI severely degrades the performance of the S&C Algorithm. To mitigate the CCI effect, a pre-filter technique based on least mean square (LMS) adaptive noise cancellation (ANC) is proposed to remove the CCI and improve the performance of the S&C Algorithm. As the simulation results show, the performance of the S&C Algorithm in the presence of severe CCI has been greatly improved especially for SIR ranges from 0 dB to 10 dB.**

I. Introduction

HetNet is an attractive approach to increase mobile network capacity. As a combination of large and small cells, HetNet consists of the existing macro base station (BS) deployment that typically transmits at high power and the added small cell BSs deployment which transmits at relatively low power, such as pico BSs, distributed antennas, femto BSs, and relays. According to the traffic forecasts, more and more small cell BSs will be required in the future.

Generated by the reuse of the same frequency between macrocell and small cells, CCI is one of the most serious problem of the HetNet, which seriously affects the user experience of the entire macro network. The crucial CCI problem deteriorates the symbol synchronization of the OFDM based networks. Symbol synchronization refers to the task of finding the starting point of a received OFDM symbols [1], which is crucial to avoid Inter-symbol interference (ISI) and inter channel interference (ICI).

There have been multiple analyses in the literature on the effect of CCI on symbol synchronization of the OFDM system. OFDM synchronization techniques can be classified into two categories: non data-aided and data-aided. The non data-aided methods make use of the correlation between the cyclic prefix (CP) and the end of the symbol; the data-aided methods make use of additional data such as preamble and pilot tones.

Van de Beek et al. [2] proposes and analyses a method using a maximum likelihood estimator to estimate time and frequency parameters by exploiting the redundancy created by the CP. However, according to C. Williams in [3], Beek's method performs badly in a multipath channel because the CP is distorted by ISI.

Moose [4] presents an idea of using repeated data symbols for synchronization, based on which the most popular synchronization technique for OFDM systems is proposed by Schmidl and Cox [5]. They design a repetitive-structure training symbol with two identical halves in time-domain. By searching for the peak of the designed timing metric, we can find the optimal starting point of the OFDM symbol. However, in the presence of CCI, S&C's performance is severely degraded.

Marey and Steendam [6] investigates the effect of narrowband interference (NBI) signals on the performance of the S&C symbol synchronizer. As evaluated in [6], the S&C algorithm estimator works well at high SIR; however the probability of missing a training sequence dramatically increases as SIR drops, which means the S&C algorithm estimator is inapplicable in the presence of CCI. However, [6] does not propose any solutions to mitigate the effect of CCI problem.

This paper proposes a method based on the S&C Algorithm to deal with the serious CCI problem generated by the HetNet. Matlab simulations are performed to model a mixed macro-small cells HetNet so as to investigate the CCI effect in a very realistic scenario. A pre-filter for S&C algorithm based symbol synchronization is designed to mitigate the impact of CCI. Matlab simulations are carried out to evaluate the performance in the presence of CCI. As the simulation results show, the performance of the S&C Algorithm in the presence of severe CCI has been greatly improved.

II. System Model

A. System Layout

We investigate the CCI problem in a OFDM based mixed-cell dense urban scenario, including mixed macro BS, pico BS, femto BS and relay nodes. Consider Figure 1 as a dense urban area with one macro BS and a number of small cell BSs with a coverage of 300 m and 30 m, respectively. The number of the small cell BSs is 50 and up to 4 UEs can be connected

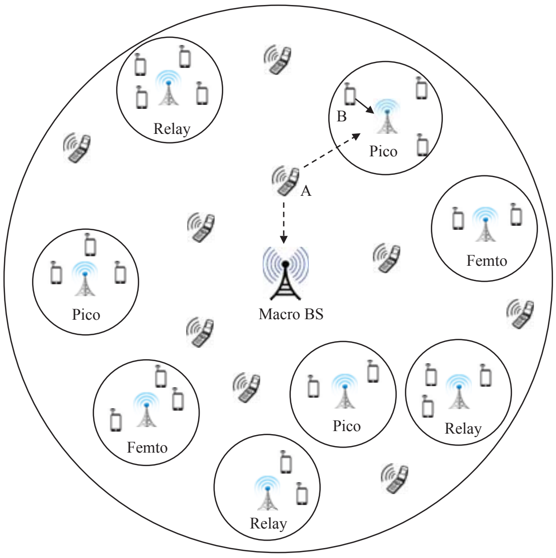

Fig. 1. Deployment of HetNet [7].

to each small cell BS. The number of the UEs covered by each BS is randomly chosen from 1 to 4. In uplink, a macro user equipment (UE) A is trying to transmit with its corresponding macro BS using subchannel L, illustrated as dotted line in the figure. Subchannel L is also allocated to a neighbouring pico UE B which is also transmitting with its pico BS at the same time, denoted as solid line. CCI occurs at this neighbouring pico BS. The effect of CCI is evaluated by calculating per-subcarrier signal to interference and noise ratio (SINR) which is given by [8]

$$SINR\left(n\right) = \frac{\frac{P_{T_x}G_{T_x}G_{R_x}}{PL_1}\left|H\left(n\right)\right|^2}{\sum_{j=1}^{J}\frac{P_{T_x}(j)G_{T_x}G_{R_x}}{PL_2(j)}\left|H_j\left(n\right)\right|^2+\sigma^2\left(n\right)} \tag{1}$$

The definition of variables used above are as follows:
$SINR\left(n\right)$: SINR of the nth subcarrier.
P_{T_x}: the transmit power on the nth subcarrier from the target small cell UEs.
G_{T_x}: the transmit antenna gain of UE.
G_{R_x}: the receive antenna gain of small cell BSs.
PL_1: the pass loss between the target small cell UEs and BSs.
$H\left(n\right)$: the channel gain of the target small cell UEs on the nth subcarrier.
J: the total number of interferers.
$P_{T_x}\left(j\right)$: the transmit power on the nth subcarrier from the jth interferer.
$PL_2\left(j\right)$: the pass loss between the jth interferer and the target small cell BS.
$H_j\left(n\right)$: the channel gain from the jth interferer to the target small cell BS on the nth subcarrier.
$\sigma^2\left(n\right)$: the Gaussian noise power on the nth subcarrier.

B. Path Loss Model

Path loss between a macro BS and its covered macro UEs can be calculated as follows [9]:

$$PL_1 = 15.3 + 37.6\log_{10}R + L_{ow} \tag{2}$$

where R is the transmitter-receiver distance in metres and L_{ow} is the penetration loss of an outdoor wall, which is 10 dB. If macro UE is outside the house, the third term is ignored.

Path loss between a small cell BS and its connected UEs can be calculated as follows [9]

$$\begin{aligned} PL_2 = {} & 38.46 + 20\log_{10}R + 0.7d_{2D,indoor} \\ & + 18.3n^{\frac{n+2}{n+1}-0.46} + qL_{iw} \end{aligned} \tag{3}$$

where $d_{2D,indoor}$ is the indoor horizontal path-length, n is the number of penetrated floors, q is the number of walls separating apartments between UE and femto BS and L_{iw} is the penetration loss of the wall separating apartments, which is 5 dB. q is uniformly chosen from the set $\{0, 1, \ldots, \left\lfloor \frac{R}{d_w} \right\rfloor\}$, where d_w represents the minimum wall separation and is assumed to be $4\ m$. The term $0.7d_{2D,indoor}$ denotes penetration loss due to walls inside an apartments.

Path loss between a small cell BS and the UEs that are not connected to it can be calculated as follows [9]

$$\begin{aligned} PL_1 = {} & \max\left(15.3 + 37.6\log_{10}R, 38.46 + 20\log_{10}R\right) \\ & +0.7d_{2D,indoor} + 18.3n^{\frac{n+2}{n+1}-0.46} + qL_{iw} + L_{ow} \end{aligned} \tag{4}$$

The function max makes sure that the path loss is not smaller than the corresponding free space loss. To maintain clarity and simplicity, we leave aside the loss caused by the walls and the floors inside an apartments.

III. Symbol Synchronization of OFDM

A. S&C Algorithm

S&C Algorithm is the most popular synchronization method for OFDM. The training symbol can be generated by transmitting a pseudonoise (PN) sequence on the even subcarriers while zeros on the odd subcarriers in frequency domain. After taking IDFT, the repetitive-structure training symbol in time domain can be written as

$$\begin{aligned} s\left(n\right) &= \frac{1}{\sqrt{N}}\sum_{k=0}^{N-1} c\left(k\right)e^{j2\pi nk/N}, \ -N_g \le n \le N-1 \\ &= \frac{1}{\sqrt{N}}\sum_{p=0}^{N/2\ -1} c_{even}\left(p\right)e^{-j\frac{2\pi}{N/2}ln} \end{aligned} \tag{5}$$

where $c\left(k\right)$ is the frequency domain training symbol, $c_{even}\left(p\right)$ is the PN sequence on the even subcarriers and $s\left(n\right)$ is the time domain training symbol. From (5) we have two identical halves as $s\left(n\right) = s\left(n+N/2\right)$ when $0 \le n \le N/2-1$. The time domain training symbol has a Cyclic Prefix (CP) of length T_g. The CP, longer than the channel impulse response, is appended to avoid the ISI.

We denote $\mathbf{h} = \left[h\left(0\right), h\left(1\right), \ldots, h\left(L-1\right)\right]^T$ the discrete channel impulse response of a Rayleigh multipath channel with L taps. After passing through the channel and discarding the CP, the received samples is expressed by [10]

$$r(n) = e^{j2\pi\varepsilon k/N} \sum_{l=0}^{L-1} h(l) s(n-\theta-l) + w(n) \qquad (6)$$

where $\theta = \lfloor \tau/T_s \rfloor$ is the timing delay normalized to the data symbol period $T_s = T/N$, $\varepsilon = f_d N T_s$ denotes the frequency offset f_d normalized to the subcarrier spacing $1/(NT_s)$, and $w(n)$ is the noise contribution. With a window of N samples, a timing metric can be define as [5] $M(d) = |P(d)|^2/[R(d)]^2$ with

$$P(d) = \sum_{m=0}^{N/2-1} \left(r^*(d+m) r(d+m+N/2)\right) \qquad (7)$$

and

$$R(d) = \sum_{m=0}^{N/2-1} |r(d+m+N/2)|^2 \qquad (8)$$

where d is the starting point of the window The receiver keeps calculating the metric $M(d)$ to find its peak. By doing so we can identify the optimal starting point of the OFDM training symbol. The resulting timing estimate is thus given by $\hat{\theta} = \arg\max_d \{M(d)\}$.

IV. CCI Impact on S&C Algorithm

A. CCI Modelling

To make the best use of the spectrum, we assume that 100% of the available spectrum is allocated to each small cell BS. This, however, may cause strong CCI problem to the entire network. When there is CCI in the network, (6) becomes

$$r(n) = e^{j2\pi\varepsilon k/N} \sum_{l=0}^{L-1} h(l) s(n-\theta-l) + w(n) + +i(n) \quad (9)$$

To fully exploit the channel frequency diversity, we randomly select subcarriers for each UE of macro cell and small cells. The location of small cell BSs are randomly distributed inside the macro cell coverage with a minimum distance of 15 m to each other. We consider uplink scenario here. Other simulation parameters are summarized in Table I.

TABLE I
Simulation Parameters

Parameter	Value
macrocell radius	300 m
subcell radius	25 m
FFT size	1024
number of data subcarriers	720
number of macro UEs	60
number of small cell BSs	10 and 50
small cell BS used fraction of spectrum	100%
small cell BS antenna gain	2 dBi
UE transmit power	23 dBm
UE antenna gain	0 dBi

Figure 2 shows a snapshot of the $SINR$ on each subcarrier. It is clear that CCI has a significant impact on the entire channel. The corruption due to the CCI becomes worse as the number of small cell BSs grows, which means the study target receives more interference. In the S&C Algorithm, the phase

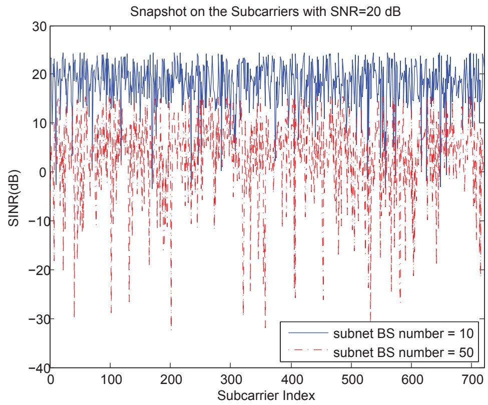

Fig. 2. Snapshot of the $SINR$ on each subcarrier.

difference between the two halves of the training symbol is $\phi = \pi\varepsilon$, which has no impact on the computation of the timing metric $M(d)$. However, the noise and CCI contributions $w(n)$ and $i(n)$ will damage the repetitive structure of the designed training symbol, resulting in wrong detection of symbol timing.

B. Statistical Properties of the Timing Metric in the Presence of CCI

In this section, we calculate the mean and variance of the timing metric of S&C Algorithm based on the analysis of narrow-band interference in [6]. A threshold λ is selected for the detection of the arrival of the training symbol. When $M(d)$ exceeds λ, it indicates the arrival of the training symbol. If a training symbol arrives but $M(d)$ does not exceed λ, miss detection occurs. If no training symbol comes but $M(d)$ is greater than λ, the timing estimator detects an arrival of the training symbol while there is none, which is called false alarm. We will focus on miss detection as the probability of false alarm is approximately equal to zero as shown by [6]. To find the probabilities of miss detection and false alarm, we need to know the statistical properties of the timing metric.

The received training sample can be written as $r(m) = s(m) + i(m) + w(m)$ where $s(m)$ is the useful signal, $i(m)$ is the CCI component, $w(m)$ is the Gaussian noise and m is the timing index. Let the variance of the real and imaginary parts of the useful signal, the inference component and the Gaussian noise component be σ_s^2, σ_i^2 and σ_n^2, respectively. When SNR and SIR is sufficiently large, the imaginary parts of $P(d)$ can be neglected, and we have $|P(d)| = \alpha + \beta$ and $|R(d)| = \alpha + \gamma$ where α, β and γ are given as [6]

$$\alpha = \sum_{m=0}^{N/2-1} \{\mathrm{Re}\{s^*(m_x) r(m_y)\} + j\,\mathrm{Im}\{s^*(m_x) s(m_y)\}\} \qquad (10)$$

$$\beta = \sum_{m=0}^{N/2-1} \mathrm{Re}\{[i^*(m_x) + w(m_x)] r(m_y)\} \qquad (11)$$

$$\gamma = \sum_{m=0}^{N/2-1} \operatorname{Re}\left\{\left[i^*\left(m_y\right)+w^*\left(m_y\right)\right] r\left(m_y\right)\right\}$$
$$+ 2\sum_{m=0}^{N/2-1} \operatorname{Re}\left\{i^*\left(m_y\right) w\left(m_y\right)\right\}$$
$$+ \sum_{m=0}^{N/2-1} \left\{\left|w\left(m_y\right)\right|^2+\left|i\left(m_y\right)\right|^2\right\} \qquad (12)$$

where $m_x = d+m$ and $m_y = d+m+N/2$. According to the central limit theorem, α, β and γ are all Gaussian random variables when N is large. We further calculate the mean of α as $\mu_\alpha = N\sigma_s^2$. Similarly, the mean and variance of β can be calculated as $\mu_\beta = 0$ and $\sigma_\beta^2 = N\left[\sigma_s^2\left(\sigma_i^2+\sigma_n^2\right)+\left(\sigma_i^2+\sigma_n^2\right)^2\right]$. The mean and the variance of σ can be calculated as $\mu_\gamma = N\left(\sigma_i^2+\sigma_n^2\right)$ and $\sigma_\gamma^2 = N\left[\sigma_s^2\left(\sigma_i^2+\sigma_n^2\right)+2\left(\sigma_i^2+\sigma_n^2\right)^2\right]$.

Define $q = \sqrt{M\left(d_{opt}\right)} = \left|P\left(d_{opt}\right)\right|/R\left(d_{opt}\right)$ where d_{opt} is the optimum timing point and q can be approximated as a Gaussian random variable with mean and variance given as [11]

$$\mu_q \approx \frac{\mu_\alpha+\mu_\beta}{\mu_\alpha+\mu_\lambda} \qquad (13)$$

$$\sigma_q^2 \approx \mu_q^2\left[\frac{\sigma_\beta^2}{\left(\mu_\alpha+\mu_\beta\right)^2}+\frac{\sigma_\gamma^2}{\left(\mu_\alpha+\mu_\gamma\right)^2}\right] \qquad (14)$$

Hence, the timing metric $M\left(d\right)$ also follows the Gaussian distribution [11] as $M\left(d\right) \approx \mu_q^2 + 2\mu_q N\left(0,\sigma_q^2\right)$ where $N\left(x,y\right)$ is a Gaussian random variable with mean x and variance y. We calculate the mean and the variance of $M\left(d\right)$ as follows

$$\mu_M \approx \left(\frac{\sigma_s^2}{\sigma_s^2+\sigma_i^2+\sigma_n^2}\right)^2 \qquad (15)$$

$$\sigma_M^2 = \frac{4\sigma_s^4\left[\left(1+\mu_M\right)\sigma_s^2\left(\sigma_i^2+\sigma_n^2\right)+\left(1+2\mu_M\right)\left(\sigma_i^2+\sigma_n^2\right)^2\right]}{N\left(\sigma_s^2+\sigma_i^2+\sigma_n^2\right)^4} \qquad (16)$$

We can calculate the probability of miss detection with a given threshold λ as [11]

$$P_{md}\left(\lambda\right) = 0.5\,\operatorname{erfc}\left(\frac{\mu_M-\lambda}{\sqrt{2\sigma_M^2}}\right) \qquad (17)$$

where $\operatorname{erfc} = 2/\sqrt{\pi}\int_x^\infty e^{-z^2}\,\mathrm{d}\,z$.

C. Effect of CCI on S&C

We carry out simulations to investigate the effects of the CCI on the the S&C Algorithm. The modulation scheme is QPSK OFDM with the FFT size of 1024 and the CP length of 64. The number of Rayleigh multipath channel taps $L = 10$. The CCI is generated as described in Section IV-A with the simulation parameters in Table I with 50 small cell BSs. For each SIR value, the simulation was run for 10000 times.

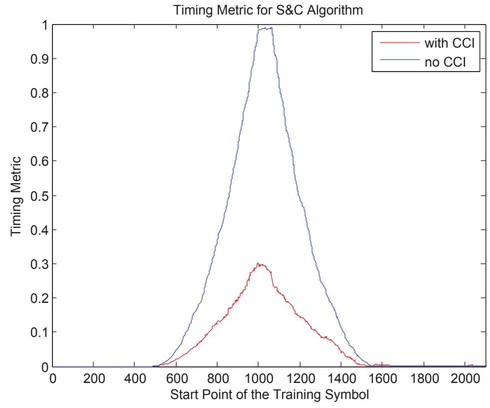

Fig. 3. Timing metric with CCI.

Figure 3 shows the timing metrics corrupted by the CCI. We can see that the maximum is greatly reduced as the repetitive structure of the training symbol is damaged by the CCI, which causes the increase of the probability of miss detection. As a consequence, in the presence of serious CCI, the S&C Algorithm is inapplicable.

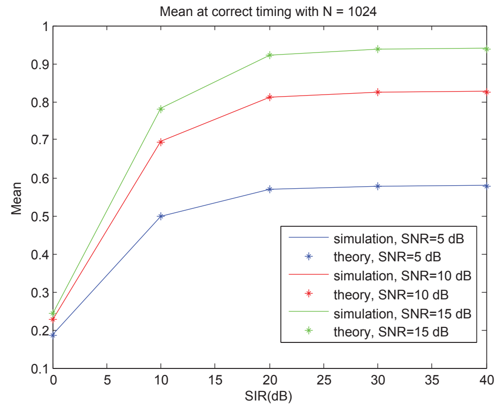

Fig. 4. Mean of the timing metric at correct timing position.

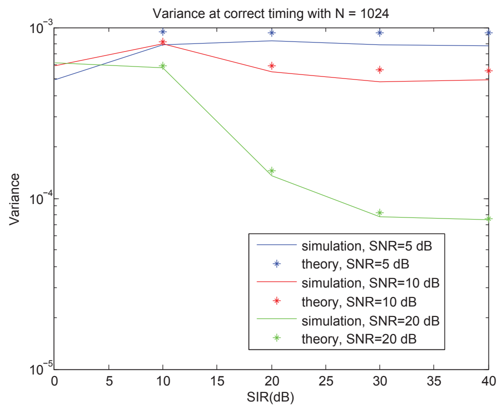

Fig. 5. Variance of the timing metric at correct timing position.

According to the analysis of [6], the statistical properties of the S&C timing metric at optimum timing point only depend on the total SIR rather than SIR per interferer. In this simulation, we randomly generate the CCI on each subcarrier and the total SIR can be written as $SIR_{total} = 1/\sum_{n=1}^{N} 1/SIR\left(n\right)$ where $SIR\left(n\right)$ is the signal-to-interference ratio on each subcarrier.

As shown in Figure 4, the simulated plots and the theoretical results are well matched. The theoretical results are calculated from (15) and (16). As the SIR increases, the mean of the timing metric is getting close to a asymptote which is determined by the value of SNR. The asymptote becomes higher with larger SNR. For the SIR ranges from 0 dB to 10 dB, the mean of the timing metric is relatively small, which causes a large probability of miss detection.

In Figure 5, with $SNR = 20$ dB, the variance of the timing metric decreases as the SIR grows. However, the variance hardly changes with the SIR and roughly remains at some certain level when SNR=5 dB and 10 dB. This is because with low SNR, the Gaussian noise component becomes a dominant factor corrupting the training symbol. Also it is worth noting that when $SNR = 5$ dB and 10 dB, the theoretical results do not perfectly agree with the simulation curves, while at $SNR = 20$ dB, the theoretical results conform very closely to the simulation curve. The reason is that the theoretical analysis is based on the assumption of sufficiently large values of SIR and SNR.

V. Pre-filtered Symbol Synchronization

A. Adaptive Filters

Adaptive filters are self-designing filters using a recursive algorithm. The most popular adaptive algorithm, the LMS algorithm is proposed by Widrow [12] and described by the following three equations [13]

Filter output:

$$y\left(n\right) = \mathbf{w}^{H}\left(n\right)\mathbf{u}\left(n\right) \tag{18}$$

Error signal:

$$e\left(n\right) = d\left(n\right) - y\left(n\right) \tag{19}$$

Tap-weight adaptation:

$$\mathbf{w}\left(n+1\right) = \mathbf{w}\left(n\right) + \mu\mathbf{u}\left(n\right)e^{*}\left(n\right) \tag{20}$$

(18) defines the computation of the filter output based on the current estimate of the tap-weight vector $\mathbf{w}\left(n\right) = \left[w_0\left(n\right), w_1\left(n\right), \cdots, w_{M-1}\left(n\right)\right]$ and the current filter input vector $\mathbf{u}\left(n\right) = \left[u_0\left(n\right), u_1\left(n\right), \cdots, u_{M-1}\left(n\right)\right]$ where n is the time index and m is the number of filter taps. (19) defines the estimation error $e\left(n\right)$. (20) defines the adaptation process of the tap-weight vector. $\mathbf{w}\left(n\right)$ represents the current estimate of the tap-weight and $\mathbf{w}\left(n+1\right) = \mathbf{w}\left(n\right) + \mu\mathbf{u}\left(n\right)e^{*}\left(n\right)$ denoted the applied adjustment. μ is the step-size parameter. The step-size parameter should satisfy the condition $0 < \mu < 2/\lambda_{\max}$ [13] where $\lambda_{\max}$ is the largest eigenvalue of the correlation matrix $\mathbf{R}$ of the filter input $\mathbf{u}$, defined as $\mathbf{R} = E\left[\mathbf{u}\left(n\right)\mathbf{u}^{H}\left(n\right)\right]$. To optimize the filter design, we choose to minimize the mean-square value of $e\left(n\right)$. Define the cost function (learning curve) as the mean square error (MSE) [13] $J\left(n\right) = E\left[\left|e\left(n\right)\right|^{2}\right]$ where E denotes the statistical expectation operator.

B. Symbol Synchronization with ANC

In this section, we apply the ANC technique to deal with the CCI problem in HetNet. As shown in Figure 6, the canceller needs two inputs, a primary input that is the corrupted received training symbol, and a reference input that is the modelled CCI signal. The reference input is adaptively filtered and subtracted from the primary input to obtain the estimated training symbol. The filtered training symbol is fed into the S&C symbol synchronization estimator to compute the timing metric. Matlab simulations are carried out and the simulation parameters are given as before. The number of filter taps $m = 20$.

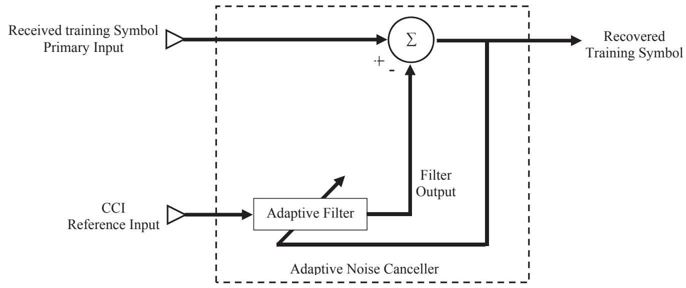

Fig. 6. Adaptive noise cancellation concept [14].

Figure 7 shows the timing metric with and without pre-filter, respectively. The CCI is generated the same way as in Figure 3. We can see that after pass through the pre-filter to remove the CCI, the received training symbol is restored from the serious corruption. Timing metric calculated after filtering can be used to search the peak which indicates the start point of the training symbol.

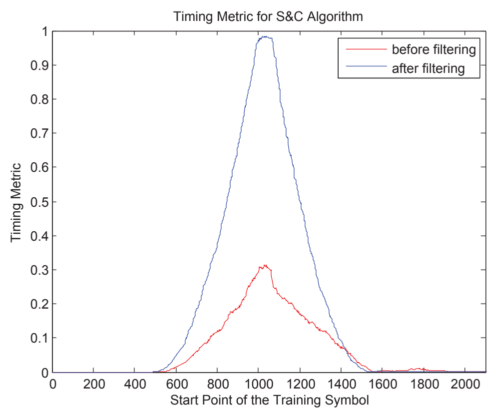

Fig. 7. Timing metric before and after filtering.

Figure 8 shows the improvement of the mean at the optimum timing position. With the pre-filter, the mean gets the raise particularly when the SIR ranges from 0 dB to 10 dB. The effect of low SIR is greatly mitigated by the pre-filtering, as we can see that the mean is improved to a relatively large value for the entire SIR range. For SNR = 20 dB, the filter still provides a decent improvement when SIR ranges from 0 dB to 10 dB. For large SIR, the improvement becomes less significant as the pre-filter reaches its performance limit.

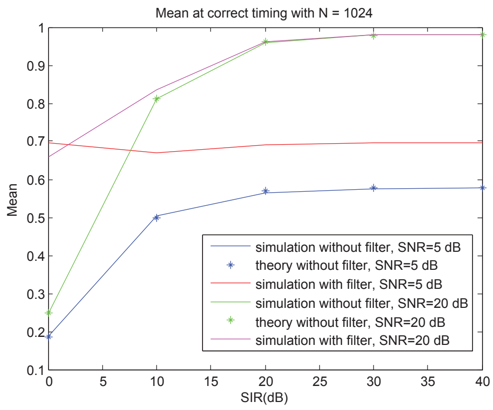

Fig. 8. Mean of the timing metric at correct timing position with filter.

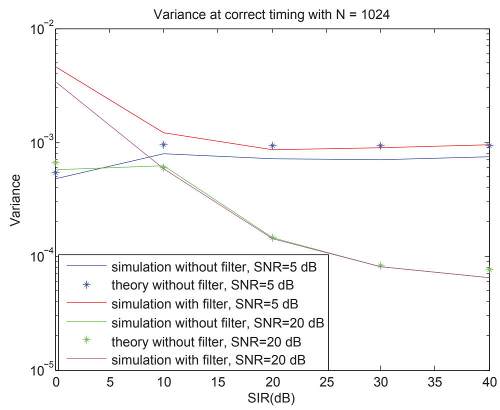

Fig. 9. Variance of the timing metric at correct timing position with filter.

It is interesting to notice that in Figure 9 the variance becomes larger with filter especially when the SIR ranges from 0 dB to 10 dB. It indicates that the timing metric after filtering is very spread out from the mean which is greatly increased.

Figure 10 displays the probability of miss detection with threshold $\lambda = 0.6$ and SIR ranging from 0 dB to 10 dB. The result shows that the P_{md} strongly depend on the strength of the CCI. As illustrated with low SIR the P_{md} remains 1, which means the S&C symbol synchronization is not working at all. There is a significant improvement of P_{md} after the pre-filter is applied. It is convincing that the method proposed here is effective in improving the performance of S&C Algorithm in the presence of severe CCI.

VI. Conclusion

This paper investigates the symbol synchronization in the presence of CCI of OFDM based HetNet. We modelled the

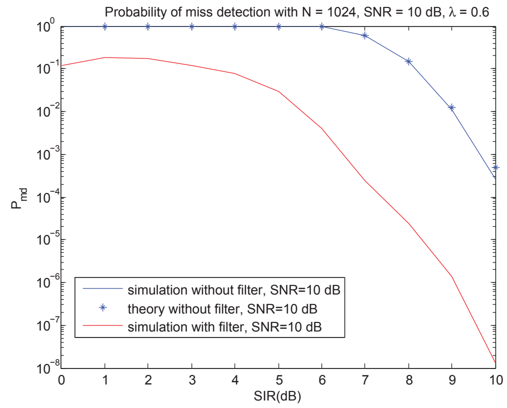

Fig. 10. Probability of miss detection after filtering.

CCI in HetNet environment of a dense urban area and matlab simulations are completed to investigate the $SINR$ on each subcarrier. We focus on the S&C Algorithm and find the performance is seriously corrupted with HetNet CCI. We find that when the SIR ranges from 0 dB to 10 dB the S&C estimator does not work properly due to the large probability of miss detection. A pre-filter is designed to remove the effect of CCI and improve the performance of the S&C Algorithm.The simulation are carried out to demonstrate the effectiveness of this pre-filter method. The performance of the S&C Algorithm in the presence of severe CCI problem has been greatly improved as the simulation results show.

References

[1] J. Heiskala and J. Terry, *OFDM Multicarrier Wireless Networks*. Sams, 2001.

[2] J.-J. van de Beek, M. Sandell, and P. O. Borjesson, "ML estimation of time and frequency offset in OFDM systems," *IEEE Transactions on Signal Processing*, vol. 45, pp. 1800–1805, 1997.

[3] C. Williams, S. McLaughlin, and M. A. Beach, "Robust ofdm timing synchronisation," *Electronics Letters*, vol. 41, pp. 751–752, 2005.

[4] P. H. Moose, "A technique for orthogonal frequency division multiplexing frequency offset correction," *IEEE Transactions on Communications*, vol. 42, pp. 2908–2914, 1994.

[5] T. M. Schmidl and D. C. Cox, "Robust frequency and timing synchronization for OFDM," *IEEE Transactions on Communications*, vol. 45, pp. 1613 – 1621, 1997.

[6] M. Marey and H. Steendam, "Analysis of the narrowband interference effect on OFDM timing synchronization," *IEEE Transactions on Signal Processing*, vol. 55, pp. 4558 – 4566, 2007.

[7] B. Li, "An effective inter-cell interference coordination scheme for heterogeneous network," in *Vehicular Technology Conference (VTC Spring)*, 2011.

[8] J. Peng, L. Zhang, and D. McLernon, "Timing synchronization for OFDMA femtocells in the presence of co-channel interference," in *Wireless Communications and Mobile Computing Conference*, 2012.

[9] the Femto Forum, "Interference management in OFDMA femtocells," the Femto Forum, Tech. Rep., 2010.

[10] M. Morelli, C.-C. J. Kuo, and M.-O. Pun, "Synchronization techniques for orthogonal frequency division multiple access (OFDMA): A tutorial review," *Proceedings of the IEEE*, vol. 95, pp. 1394 – 1427, 2007.

[11] R. E. Walpole, R. H. Myers, S. L. M. (Author), and K. E. Ye, *Probability and Statistics for Engineers and Scientists*. Pearson, 2011.

[12] B. Widrow and M. E. Hoff, "Adaptive switching circuits," in *IRE WESCON Convention Record*, 1960.

[13] S. Haykin, *Adaptive Filter Theory*, T. Kailath, Ed. Prentice-Hall, 2002.

[14] *Adaptive noise cancelling: Principles and applications*, vol. 63, IEEE. Proceedings of the IEEE, 1975.